Sensing of nanostructured CdS thin films via several solution concentrations

R. I. Jasim [a], E. H. Hadi [a], A. A. Mansour [b], S. A. Hussein [c], S. S. Chiad [a,*], N. F. Habubi [d], Y. H. Kadhim [e], M. Jadan [f,g]

[a] *Department of Physics, College of Education, Mustansiriyah University, Iraq*
[b] *Ministry of Education, Directorate of Education Baghdad Governorate, Al-Karkh third, Iraq*
[c] *Department of Medical Laboratory Techniques, Al-Manara College for Medical Science, Iraq*
[d] *Department of Radiology Technologies, Al-Nukhba, University College, Baghdad 10013, Iraq*
[e] *Department of Optics Techniques, College of Haelth and Medical Techniques, AL-Mustaqbal University, Babylon, Hillah, 51001, Iraq*
[f] *Department of Physics, College of Science, Imam Abdulrahman Bin Faisal University, P.O. Box 1982, 31441 Dammam, Saudi Arabia*
[g] *Basic and Applied Scientific Research Center, Imam Abdulrahman Bin Faisal University, P.O. Box 1982, 31441 Dammam, Saudi Arabia*

Using chemical bath deposition (CBD) methods and various molarities, nanostructured CdS thin films were developed. XRD assured that these films were cubic polycrystalline, containing larger grains as the solution's concentration of cadmium ions increased. Dislocation density values dropped from 79.32 to 62.90 as a result, nevertheless. Also, the strain is lowered from 30.88 to 27.50. AFM results demonstrate that these films suffer a decrease in the value of average particle size, root mean square, and roughness with the molarity concentration. SEM images show CdS thin films at various molarities (0.10, 0.15, 0.20) M, indicating reduced grain size with increased concentration. The optical characteristics indicate a large band gap decreases from 2.46 eV to 2.34 eV and a high transmittance in the visible portion of the spectrum of more than 97.5%. The Refractive Index value changed from 3.23 to 3.11 as the content of cadmium ions increased. CdS films show p-type behavior, reducing resistance with NO_2 gas, influenced by molar concentration. The sensitivity of CdS films to NO_2 shows a decrement with increased molar concentrations.

(Received September 29, 2024; Accepted January 10, 2025)

Keywords: Cadmium sulfide, Thin films, Solution concentration, Structural, Morphological and optical properties, Band gap

1. Introduction

Due to their electrical and optical characteristics, semiconducting materials draw much attention, and numerous optoelectronic applications, such as LED and photo-transistors cadmium sulfides (CdS), have been extensively explored. At ambient temperature, the band gap of CdS is 2.42 eV [3], and it exhibits n-type semiconducting characteristics with an electrical resistivity of 10^{-2}-10^{-4} cm. Cadmium sulphides have high electrical conductivity, low resistance, and high transmittance in the visible portion of the solar spectrum. [4]. In recent years, the fabrication of electronic and optoelectronic devices has shown a strong interest in CdS thin films [5-7]. Many physical and chemical deposition methods, such as CBD [8–10], Chemical Spray Pyrolysis (CSP) [11, 12], Molecular Beam Epitaxy (MBE) [13], and sol-gel [14,15]. have been used to create CdS thin films. The CBD technique offers many benefits over other approaches, including its simplicity, lack of need for expensive equipment, minimal material waste, cost-effective manner to deposit

* Corresponding author: dr.sami@uomustansiriyah.edu.iq
https://doi.org/10.15251/CL.2025.221.43

material across a vast region, and lack of handling dangerous gases. Because the CBD approach is a lengthy procedure, the crystallites' better alignment and improved grain structure are possible [9].

The CBD approach is a simple, inexpensive process that is especially helpful for industrial applications involving huge areas, which is why it has recently seen a lot of use. High-quality films are produced using the CBD technique, which changes the pH, temperature, and reagent concentrations. With the help of XRD, AFM, and a UV-visible spectrophotometer, the films were evaluated to determine the Influence of solution concentration on several physical features of thin films made of cadmium sulfide.

2. Experimental

Glass bases have thin sulphide coatings through chemical bath deposition. The bases were dried at 80°C in an oven after being cleaned with distilled water, HCl, and detergent. [$Cd(NO_3)_2.4H_2O$] with 0.05 M to 0.2 M as a source of (Cd^{+2}) ions, and 0.1 M thiourea [$SC(NH_2)_2$] as a source of (S^{2-}) were used to develop the CdS thin films on a glass base. To bring the pH to 10, 25% ammonia hydroxide solution (NH_4OH) was gradually added. For around 10 minutes, the solution was agitated to achieve uniform dissolution. The bath was held at 70°C for three hours without being disturbed. When the CdS films were deposited, they were ultrasonically cleaned with methanol to remove any weakly attached CdS particles before being annealed in the air for an hour. At 673 K, using a furnace model called the Yamato FM 27. In the investigation of film characteristics, film thickness is a crucial factor. The gravimetric Equation t=m/(A) is used to measure thickness where m is the film's mass in grams, A is its area in square centimeters, and is the material's bulk density (CdS = 4.69 g/cm^3) [17]. CdS thin films could be as thick as 680 nm. The X-ray 6000 (Shimadzu) diffractometer was used to perform the XRD study at 40 kV and 30 mA. AFM was employed to study the surface morphology of the films. The optical transmission spectra were examined using UV-visible spectrophotometer (Cintra 5) GBC-Astrural.

3. Results and discussions

Figure 1 displays the deposited films' XRD patterns. When compared to JCPDS CARD: 21-0829, the diffraction peaks noted in XRD patterns of all films are peaks at 28.31°, 32.62°, 47.14°, and 58.53° label to the (111), (200), (220), and (222) planes, respectively, of cubic crystal structure of CdS thin films. As the films become polycrystalline, distinct concentration molarity patterns become visible. The XRD pattern of various concentration molarities reveals that all films have a preferred orientation along the (111) plane. At increasing concentration molarity, the intensities of the diffraction peak of the (111) plane tended to rise significantly. This behavior includes an increase in the crystallites' preferred orientation due to the effects of concentration molarity. [23].

The Grain size (D) is acquired via Scherrer formula [24, 25]:

$$D = \frac{K\lambda}{\beta cos\theta} \tag{1}$$

where k = 0.94, λ is the X-ray wavelength, β is FWHM, and θ is the reflection angle [26]. According to Figure 3, the diffraction peaks get sharper and more intense as the cadmium ion concentration rises, indicating that the grains get bigger and the crystal quality is better. D go from 11.22 nm to 12.60 nm. These findings concur with other research that has been published, such as research [27, 28].

The Dislocation density (δ) was determined by computing Equation (2) [29,30];

$$\delta = \frac{1}{D^2} \tag{2}$$

and was found that the dislocation density decreased from 179.32 to 62.90 nm with the increasing cadmium ion concentration.

The strain (Ɛ) was determined by computing Equation (3) [31, 32]:

$$\varepsilon = \frac{\beta \cos\theta}{4} \quad (3)$$

In addition, as the concentration of cadmium ions rises, strain (Ɛ) falls from 30.88 to 27.50. The structural parameters P_{st} are shown in Figure 2. The average size and other factors indeed have an inverse connection.

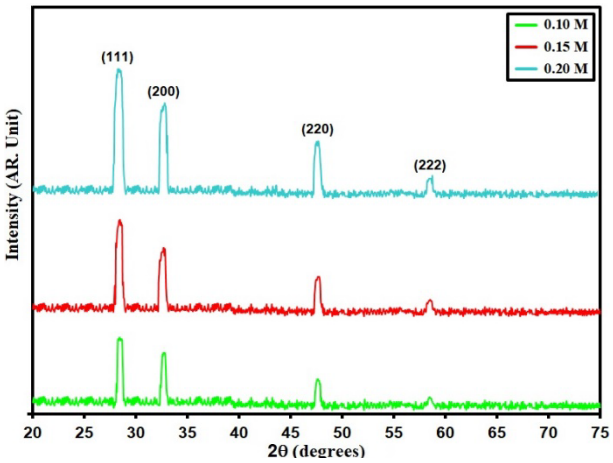

Fig. 1. XRD styles of grown films.

Table 1. D, E_g and P_{st} of grown films.

Sample (M)	2 θ (°)	(hkl) Plane	FWHM (°)	E_g(eV)	*D* (nm)	δ (× 10^{14}) (lines/m^2)	ε × 10^{-4}
0.10	28.31	111	.0.73	2.46	11.22	79.32	30.88
0.15	28.29	111	0.69	0.69	11.87	70.87	29.18
0.20	28.26	111	0.65	0.65	12.60	62.90	27.50

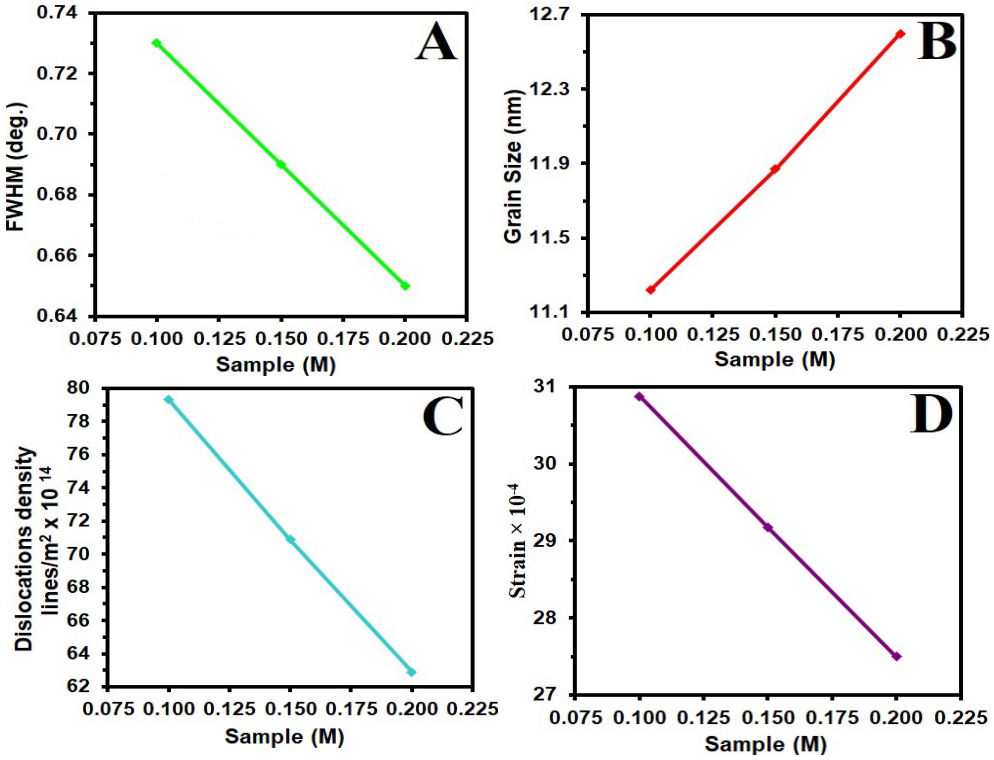

Fig.2. P_{st} of the grown films.

AFM pictures of a glass substrate exposed to various concentrations of CdS are shown in Fig (3). The 3D-AFM images in Fig. 3 show that the grains are evenly distributed throughout the 10 nm x 10 nm scanning region, with distinct grains reaching upward. This surface property is crucial for solar cells and photodetectors, according to Anwar et al. [33], Ezekoye [34], and Islam et al. [35]. The image also shows that film was continuous with extremely well-connected grains free of pinholes, fissures, and big clusters. The majority of submicron particles have relatively coarse surfaces and are composed. Dergacheva and others [36]. AFM pictures and cross-sections with surface roughness Ra values between 5.07 and 2.33 nm and root mean square RMS values between 7.03 and 3.14 nm indicate the production of thin films on a glass base, as offered in Fig. 3. RMS values were reported by Olofinjan et al. to be less than 50 nm [37], showing smooth films. However, the current investigation results show that R_a and RMS varied with molarity concentration. Thus, as the molarity concentration increased (1.0, 1.5, and 2.0 M), the RMS, average particle size P_{av} and R_a reduced. The AFM parameters P_{AFM} at various molarity concentrations are shown in Table 2.

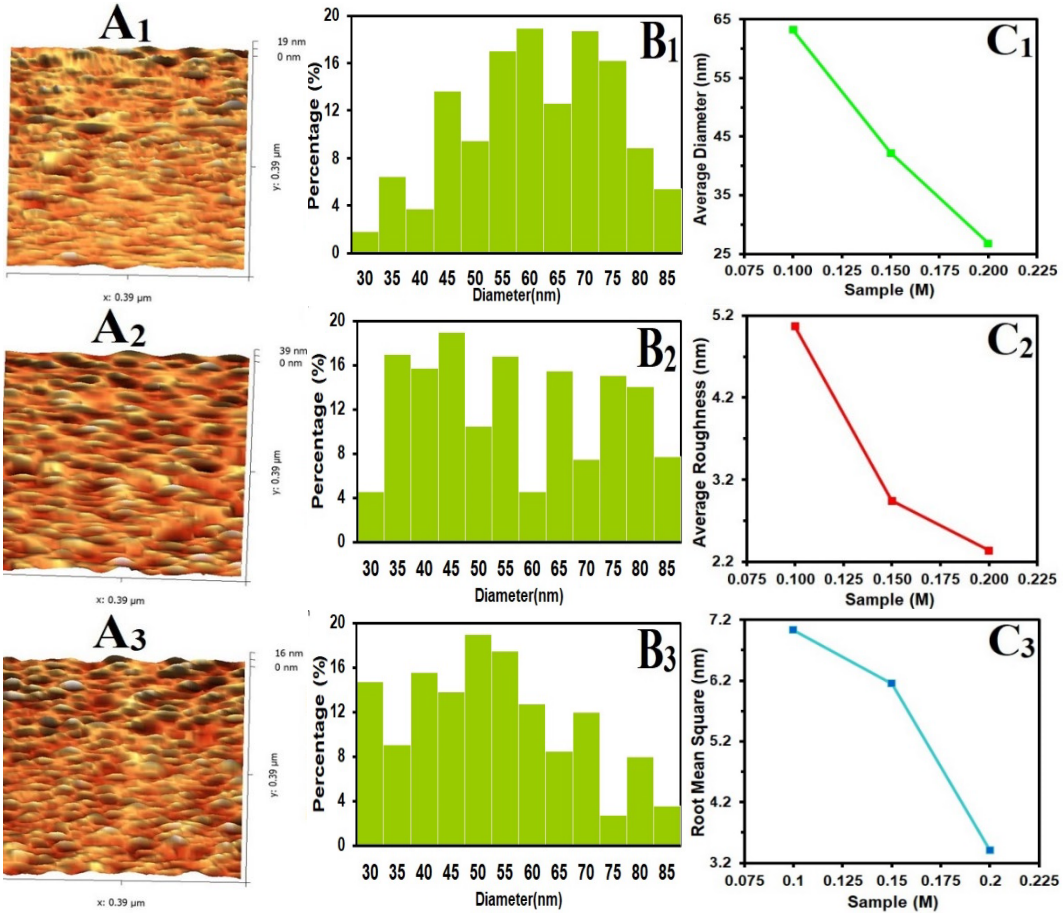

Fig. 3. AFM information.

Table 2. P_{AFM} of grown films.

Sample M	P_{av} nm	R_a (nm)	RMS (nm)
0.10	63.2	5.07	7.03
0.15	42.3	2.94	6.15
0.20	26.8	2.33	3.41

SEM images in Figure 4 (a), (b), and (c) depict the surface morphology of CdS thin films at varying molar concentrations (0.10, 0.15, and 0.20) M. Increasing concentration leads to smaller grain sizes. At (0.15 and 0.20) M, slight deviations in morphology from 0.10 M occur, likely due to differences in lattice structure and deposition-induced defects, impacting chemical processes.

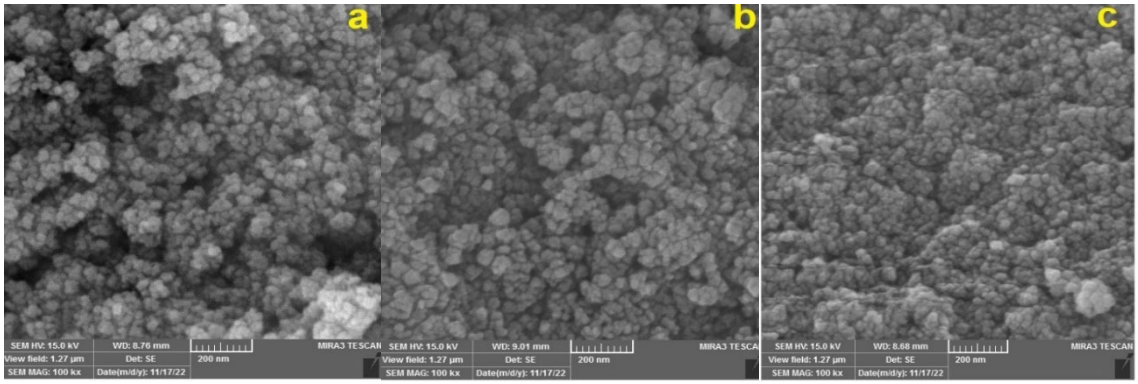

Fig. 4. SEM images of CdS: (a) 0.10 M, (b) 0.15 M, (c) 0.20 M.

The UV-spectrometer is accustomed to characterizing CdS thin films' optical properties, and the spectrum was seen between 300 and 900 nm in wavelength. Figure 5 displays the absorption spectra formed at various molarities. Absorbance rises as molarity concentration does. The spectra reveal a blue shift in the absorbance edges relative to the bulk CdS, demonstrating the quantum confinement effect in nanoparticles. [38].

The transmittance (T) of these films, illustrated in Fig. (5), was calculated from absorbance (A) data using the following [39]:

$$A = 2 - \log 10\ (\%\ T) \tag{4}$$

In Fig. 6, the transmission percentage is relatively low in the absorption spectral region at a wavelength of about 530 nm. Every single film has a strong transmission range above 500 nm. The range of visible to infrared transmission was between 93.9 and 97.5%. i.e., the film has a lower visible region transmission rate of 97.5%. While transmittance increased at wavelength (530) nm, transmittance declined as molarity increased. Three different molarity concentrations of CdS absorbance below 530 nm were determined from the UV study. It was demonstrated unequivocally that CdS nanoparticles were very suitable for optoelectronic applications. [40].

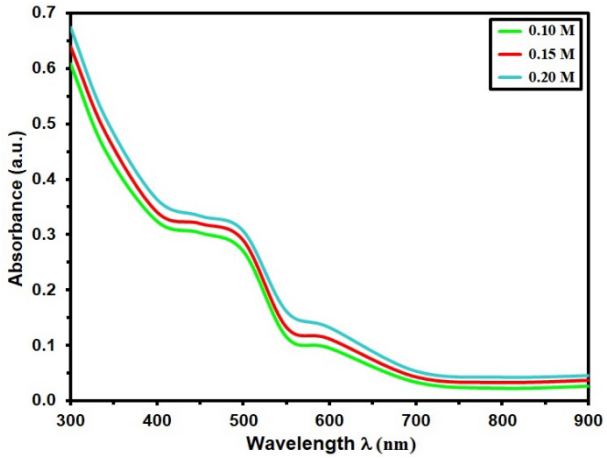

Fig. 5. A of the grown films.

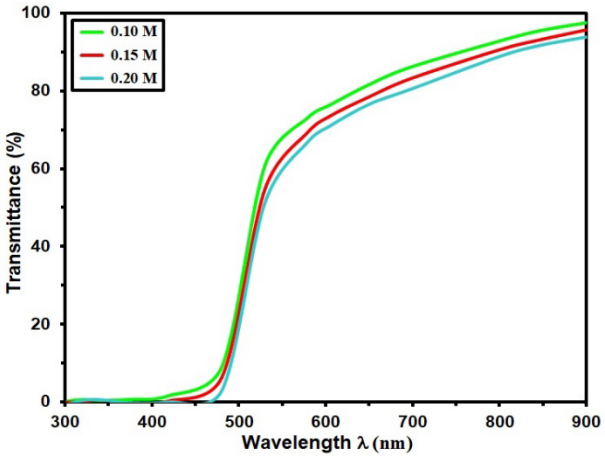

Fig. 6. T of the grown films.

The absorption coefficient α is computed from Lambert law [41]:

$$\alpha=2.303A/t \tag{5}$$

Where t is the film thickness, the films have a high α (10^4 cm^{-1}), which denotes direct electronic transitions, as shown in Fig. (7), which plots α via photon energy (hυ). It can be seen that αsomewhat increases by increasing the molarity concentration and that the absorption edge shifts towards the low energies. α increases by increasing the photon energy and rapidly increases in the region of (2.26-2.34) eV. The absorption coefficient values have increased because of the creation of new localized levels that penetrate the basic levels that absorb the low-energy photons. [42,43].

The optical band gap (E_g) was estimated via Eq. 6 [44]:

$$(\alpha h\nu) = B\left(h\nu - E_g\right)^{1/2} \tag{6}$$

where B is a constant, the relationship between $(h\upsilon)^2$ and hυ was plotted to evaluate E_g of CdS. From Fig. 8, it was discovered that E_g value of the CdS film drops from (2.46 to 2.34) eV when the cadmium molarity rises, with an increase in cadmium molarity leading to an increase in *D*. The enhancement in the film's crystallinity, or *D* and lattice characteristics, is what caused the band gap to narrow. High concentration leads to a pronounced absorption edge because films become more crystalline, and D increases with increased cadmium molarity. These figures and the values reported by others are reasonably consistent. [45, 46].

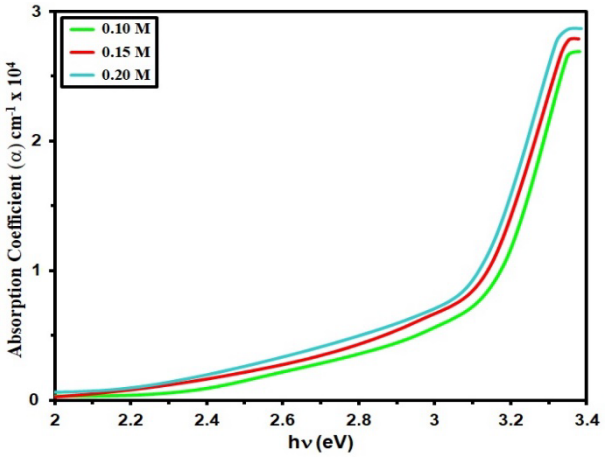

Fig. 7. α of grown films.

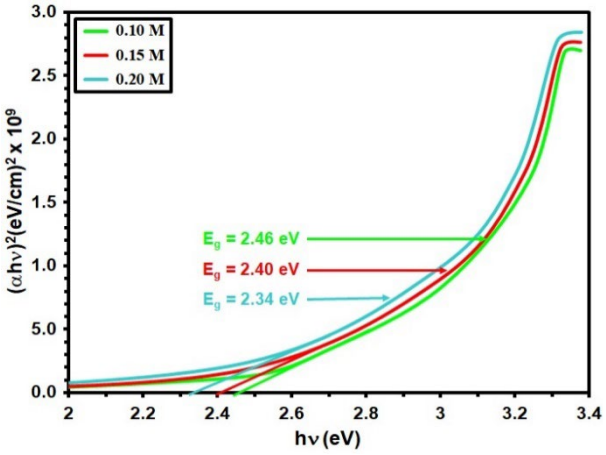

Fig. 8. E_g of deposit films.

The extinction coefficient (k) has been determined via Eq. 7 [47, 48]:

$$k = \frac{\alpha\lambda}{4\pi} \tag{7}$$

where λ is the wavelength. This Equation makes it evident that k depends on and behaves similarly to. *K* varies with molarity concentration (0.10, 0.15, and 0.20) M and wavelength, as seen in Fig. (9); as molarity concentration *K* decreases. This is attributable to the absorption coefficient growing since donor levels are associated with deeper donor levels, and the photons can absorb these levels when they become released., raising the absorbance and α Since k behaves similarly to (α) and depends on it, it will decrease as the molarity concentration increases. [49-51].

The refractive index (n) obtained via Eq. 8 [52, 53]:

$$n = \frac{1 + R^{\frac{1}{2}}}{1 - R^{\frac{1}{2}}} \tag{8}$$

where R is the reflectance. Figure 10 shows how n changes for CdS at molarities of 0.10, 0.15, and 0.20 M as a function of wavelength. This graph shows that the refractive index drops as the incident photon's wavelength increases.

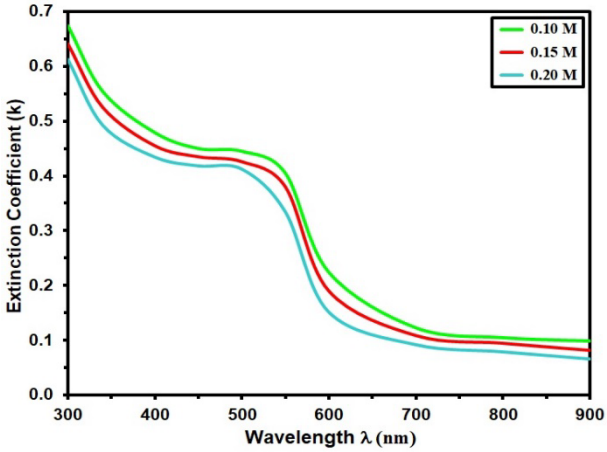

Fig. 9. (k) of grown films.

Also, the refractive index of CdS with molarity concentrations of 0.10, 0.15, and 0.20 M falls as molarity concentration increases. This decline is due to the films' shrinking grain size with increasing molarity concentration, which in turn caused an increase in the films' compactness. This decreased the speed of light in the thin film's substance, leading to the decline. [54- 56].

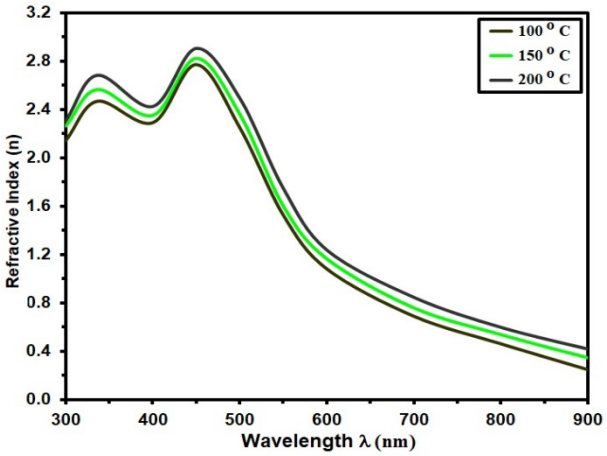

Fig. 10. n for grown films.

Fig. (11) illustrates the resistance versus response time of CdS thin films at varying molar concentrations (0.10, 0.15, and 0.20 M) were assessed for NO_2 gas at an operational temperature of 150°C. The decrease in resistance upon NO_2 gas introduction suggests CdS behaves as a p-type semiconductor. This indicates that oxidizing gases like NO_2 react with the film surface, capturing electrons from the conduction band and increasing the number of holes, thus reducing film resistance [57-59]. CdS at 0.20 M exhibits the highest resistance, highlighting the impact of molar concentrations on the semiconductor properties of the films.

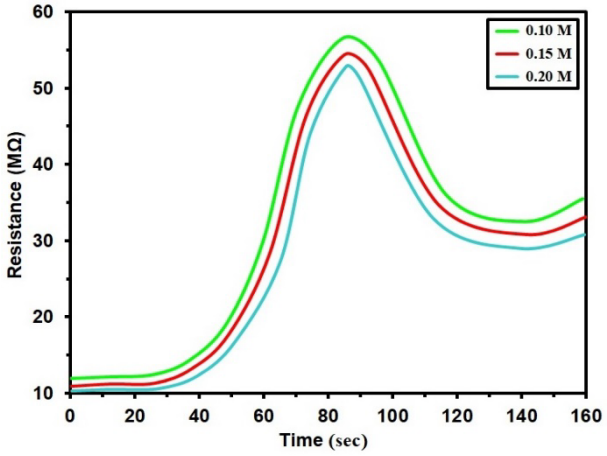

Fig. 11. Resistance versus response time of CdS thin films at varying molar concentrations (0.10, 0.15, and 0.20) M.

Sensor response can be calculated with equation [52].

$$Sensitivity = \frac{\Delta R}{R_g} = \left|\frac{R_g - R_a}{R_g}\right| \times 100\ \% \qquad (9)$$

Figure (12) illustrates the sensitivity of CdS thin films to NO_2 gas at various molar concentrations (0.10, 0.15, and 0.20 M) and NO_2 concentrations of 100, 150, and 200 ppm. Sensitivity declines with increasing molar concentrations, notably in 0.20 M films, possibly due to hindered gas diffusion [53,54]. This reduction in sensitivity across NO_2 concentrations indicates that thinner CdS films exhibit superior responsiveness to NO_2 gas.

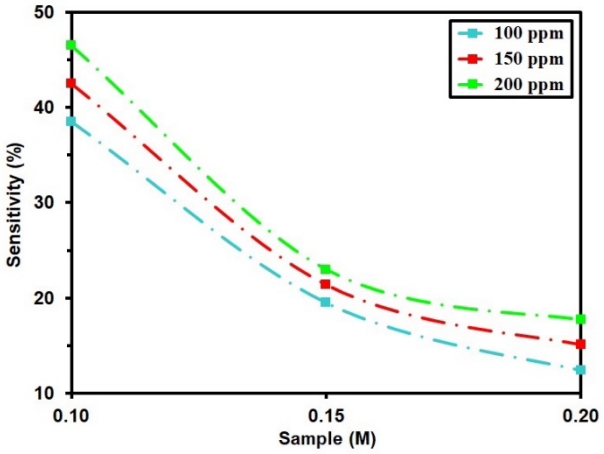

Fig. 12. Sensitivity of CdS thin films at varying molar concentrations (0.10, 0.15, and 0.20 M).

4. Conclusion

The X-ray diffraction confirmed that the nanostructured films were polycrystalline by using varying molarities via a chemical bath to deposit cadmium sulfide (CdS) thin films. A favored orientation along the (111) plane can be seen in all samples. As the concentration molarity increased, the grain size increased. The strain, was dropped from 30.88 to 27.50. Also, the same behavior was noticed in dislocation density values from 79.32 to 62.90. When the concentration molarity rises, particle size drops from 63.2 to 26.8 nm in the AFM pictures. SEM images show that increased concentration leads to smaller grain size, influencing morphology. When the concentration molarity was increased to 2.0 M, Rrms fell from 7.03 nm to 3.41 nm.

The films' high optical transmittance, 93.9-97.5%, and low reflection in the 530-900 nm wavelength range make them appropriate for usage as transparent windows in solar cells. Increasing concentration molarity lowered the optical band gap for the permitted direct transition to 2.0 M from (2.46 to 2.34) eV. (n, k) were also computed in this spectrum. CdS films show p-type behavior, and resistance decreases with NO_2. Molar concentration affects resistance. The sensitivity of CdS films to NO_2 diminishes with increasing molarity.

Acknowledgements

Mustansiriyah University and Alnukhba University College provided financial support for this project, for which the authors are grateful.

References

[1] M. Ilieva, D. Dimova-Malinovska, B. Ranguelov and I. Markov, Journal of Physics: Condensed Matter, 11 (49), 10025-10031 (1999); https://doi.org/10.1088/0953-8984/11/49/320

[2] A. Davis, K. Vaccaro, H. Dauplaise, W. Waters and J. Lorenzo, Journal of the Electrochemical Society, 146 (3), 1046-1053 (1999); https://doi.org/10.1149/1.1391719
[3] R. Mariappan, V. Ponnuswamy, M. Ragavendar, D. Krishnamoorthi, C. Sankar, Optik 123, 1098-1102, (2012); https://doi.org/10.1016/j.ijleo.2011.07.038
[4] J. Han, C. Spanheimer, G. Haindl, G. Fu, V. Krishnakumar, J. Schaffner, C. Fan, K. Zhao, A. Klein, W. Jaegermann, Sol. Energy Mater. Sol. C, 95 (3), 816-820, (2011); https://doi.org/10.1016/j.solmat.2010.10.027
[5] M. Contreras, M. Romero, B. To, F. Hasoon, R. Noufi, S. Ward and K. Ramanathan, Thin Solid Films, 403-404 (579), 204-211 (2002); https://doi.org/10.1016/S0040-6090(01)01538-3
[6] M. Fatolah, G. Khayati, P. Fatolah, J. Sulphur Chem. 43, 366 (2022); https://doi.org/10.1080/17415993.2022.2052883
[7] F. A. Jasima , Z. S. A. Mosa, N. F. Habubi, Y. H. Kadhim, S. S. Chiad, Digest Journal of Nanomaterials and Biostructures, 18 (3), 1039–1049 (2023); https://doi.org/10.15251/DJNB.2023.183.1039
[8] O. Vigil-Galan, J. Ximel-lo-Quiebras, J. Aguilar-Hernandez, G. Contreras-Puente, A. Cruz-Orea, J. Mendoza-Alvarez, J. Cardona-Bedoya, C. Ruiz and V. Bermudez, Semiconductor Science and Technology, 21, 76 (2006); https://doi.org/10.1088/0268-1242/21/1/014
[9] S. Tec-Yam, R. Pati˜no, and A. I. Oliva, Current Applied Physics 11, 914–920 (2011); https://doi.org/10.1016/j.cap.2010.12.016
[10] S. Tec-Yam, R. Pati˜no, and A. I. Oliva, Current Applied Physics, 11, 914–920 (2011); https://doi.org/10.1016/j.cap.2010.12.016
[11] Salih Yılmaz, The investigation of spray pyrolysis grown CdS thin films doped with fluorine atoms. Applied Surface Science 357, 873–879, (2015); https://doi.org/10.1016/j.apsusc.2015.09.098
[12] D. Herrera-Molina , J.E. Diosa , A. Fernandez-Perez , E. Mosquera-Vargas, Materials Science and Engineering B 273, 115451 (2021); https://doi.org/10.1016/j.mseb.2021.115451
[13] P. Boieriu, R. Sporken, Y. Xin, N. Browning and S. Sivananthan, Journal of Electronic Materials, 29 (6), 718-722 (2000); https://doi.org/10.1007/s11664-000-0212-3
[14] M.S. Sivakumar, Structural, Journal of Materials Science: Materials in Electronics, 28 (17), 12432-12439, (2017); https://doi.org/10.1080/02670844.2017.13039
[15] A. Kerimova, E. Bagiyev, E . Aliyeva, et al., Phys. Status Solidi C, 14 (6), 1600144 (2017); https://doi.org/10.1002/pssc.201600144
[16] A. S. Al Rawas, M. Y. Slewa, B. A. Bader, N. F. Habubi, S. S. Chiad, Journal of Green Engineering,10 (9), 7141-7153 (2020); https://doi.org/10.1021/acsami.1c00304
[17] R. S. Ali, H. S. Rasheed, N. F. Habubi, S.S. Chiad, Chalcogenide Letters,, 20 (1), 63–72 (2023; https://doi.org/10.15251/CL.2023.201.63
[18] A. S. Alkelaby, K. H. Abass, T. H. Mubarak, N. F. , Habubi, S. S. Chiad, I. Al-Baidhany, Journal of Global Pharma Technology 11(4), 347-352 (2019).
[19] N. Y. Ahmed, B. A. Bader, M. Y. Slewa, N. F. Habubi, S. S. Chiad, NeuroQuantology, 18(6), 55-60 (2020); https://doi.org/10.1016/j.jlumin.2021.118221
[20] A. A. Khadayeir, K. H. Abass, S. S. Chiad, M. K. Mohammed, N. F. Habubi, T. K. Hameed, I. A. Al-Baidhany, Journal of Engineering and Applied Sciences, 13 (22), 9689-9692 (2018).
[21] A. Ghazai, K. Qader, N. F. Hbubi, S. S. Chiad, O. Abdulmunem, IOP Conference Series: Materials Science and Engineering, 870 (1), 012027 (2020); https://doi.org/ 10.1088/1757-899X/870/1/012027
[22] R. S. Ali, M. K. Mohammed, A. A. Khadayeir, Z. M. Abood, N. F. Habubi and S. S. Chiad, Journal of Physics: Conference Series, 1664 (1), 012016 (2020); https://doi:10.1088/1742-6596/1664/1/012016
[23] A. A. Khadayeir, R. I. Jasim, S. H. Jumaah, N. F, Habubi, S. S. Chiad, Journal of Physics: Conference Series,1664 (1) (2020); https://doi.org/10.1088/1742-6596/1664/1/012009
[24] O. M. Abdulmunem, A. M. Jabbar, S. K. Muhammad, M. O. Dawood, S. S. Chiad, N. F. Habubi, Journal of Physics: Conference Series,1660 (1), 012055 (2020); https://doi.org/ 10.1088/1742-6596/1660/1/012055
[25] S. A. Hameed, N. A. Bakr, A. M. Hassan, A. N. Jasim, AIP Conference Proceedings, 2213, 020082 (2020); https://doi.org/10.1063/5.0000310

[26] E. H. Hadi, M. A. Abbsa, A. A. Khadayeir, Z. M. Abood, N. F. Habubi, and S.S. Chiad, Journal of Physics: Conference Series, 1664 (1), 012069 (2020); https://doi.org/ 10.1088/1742-6596/1664/1/012069
[27] B. A. Bader, S. K. Muhammad, A. M. Jabbar, K. H. Abass, S. S. Chiad, N. F. Habubi, J. Nanostruct, 10(4): 744-750, (2020); https://doi.org/ 10.22052/JNS.2020.04.007
[28] F. H. Jasim, H. R. Shakir, S. S. Chiad,N. F. Habubi, Y. H. Kadhi,, Jadan, M., Digest Journal of Nanomaterials and Biostructures, 18(4), 1385–1393 (2023); https://doi.org/10.15251/DJNB.2023.184.1385
[29] H. T. Salloom, R. I. Jasim, N. F. Habubi, S. S. Chiad, M. Jadan, J. S. Addasi, Chinese Physics B, 30 (6), 068505 (2021); https://doi.org/10.1088/1674-1056/abd2a7
[30] S. S Chiad,, A. S. Alkelaby, K. S. Sharba,, Journal of Global Pharma Technology, 11 (7), 662-665, (2020); https://doi.org/10.1021/acscatal.1c01666
[31] Chiad, S.S., Noor, H.A., Abdulmunem, O.M., Habubi, N.F., Journal of Physics: Conference Series 1362(1), 012115 (2019); https://doi.org/10.1088/1742-6596/1362/1/012115
[32] M. Ilieva, D. Dimova-Malinovska, B. Ranguelov and I. Markov, Journal of Physics: Condensed Matter, 11(49), 10025-10031 (1999); https://doi.org/10.1088/0953-8984/11/49/320
[33] K. Y. Qader, E. H. Hadi, N. F. Habubi, S. S. Chiad, M. Jadan, J. S. Addasi, International Journal of Thin Films Science and Technology, 10 (1), 41-44 (2021); https://doi.org/ 10.18576/ijtfst/100107
[34] N. N. Jandow, M. S. Othman, N. F.Habubi, S. S. Chiad, K. A. Mishjil, I. A. Al-Baidhany, Materials Research Express, 6 (11), (2020); https://doi.org/10.1088/2053-1591/ab4af8
[35] M. D. Sakhil, Z. M. Shaban, K. S. Sharba, N. F. Habub, K. H. Abass, S. S. Chiad, A. S. Alkelaby, NeuroQuantology, 18 (5), 56-61 (2020); https://doi.org/10.14704/nq.2020.18.5.NQ20168
[36] E. S. Hassan, K. Y. Qader, E. H. Hadi, S. S. Chiad, N. F. Habubi, K. H. Abass, Nano Biomedicine and Engineering, 12(3), pp. 205-213 (2020); https://doi.org/10.5101/nbe.v12i3.p205-213
[37] M. S. Othman, K. A. Mishjil, H. G. Rashid, S. S. Chiad, N. F. Habubi, I. A. Al-Baidhany, Journal of Materials Science: Materials in Electronics, 31(11), 9037-9043 (2020); https://doi.org/10.1007/s10854-020-03437-0
[38] E. H. Hadi, D. A. Sabur, S. S. Chiad, N. F. Habubi, K., Abass, Journal of Green Engineering, 10 (10), 8390-8400 (2020); https://doi.org/10.1063/5.0095169
[39] K. Y. Qader, R. A. Ghazi, A. M. Jabbar, K. H. Abass, S. S. Chiad, Journal of Green Engineering, 10 (10), 7387-7398 (2020); https://doi.org/10.1016/j.jece.2020.104011
[40] R. I. Jasim, E. H. Hadi, S. S. Chiad, N. F. Habubi, M. Jadan, J. S. Addasi, Journal of Ovonic Research, 19 (2), 187 – 196 (2023)..
[41] K. S. Sharba, A. S. Alkelaby, M. D. Sakhil, K. H. Abass, N. F. Habubi, S. S. Chiad, Enhancement of urbach energy and dispersion parameters of polyvinyl alcohol with Kaolin additive, NeuroQuantology, 18 (3), 66-73 (2020); https://doi.org/10.14704/NQ.2020.18.3.NQ20152
[42] A. A. Khadayeir, E. S. Hassan, S. S. Chiad, N. F. Habubi, K. H. Abass, M. H. Rahid, T. H. Mubarak, M. O. Dawod, I. A. Al-Baidhany, Journal of Physics: Conference Series 1234 (1), 012014, (2019); https://doi.10.88/1742-6596/1234/1/012014
[43] Hassan, E.S., Mubarak, T.H., Chiad, S.S., Habubi, N.F., Khadayeir, A.A., Dawood, M.O., Al-Baidhany, I. A. , Journal of Physics: Conference Series, 1294(2), 022008 (2019); https://doi.10.88/1742-6596/1294/2/022008
[44] M.O. Dawood, S.S. Chiad, A.J. Ghazai, N.F. Habubi, O.M. Abdulmunem, AIP Conference Proceedings 2213, 020102,(2020); https://doi.org/10.1063/5.0000136
[45] S. S. Chiad, K. H. Abass, T. H. Mubarak, N. F. Habubi, M. K. Mohammed, A. A. , Khadayeir, Journal of Global Pharma Technolog, 11(4), 369-375 (2019).
[46] S. K. Muhammad, M. O. Dawood, N. Y. Ahmed, E. S. Hassan, N. F. Habubi, S. S. Chiad, Journal of Physics: Conference Series, 1660 (1), 012057 (2020); https://doi.org/ 10.1088/1742-6596/1660/1/012057
[47] B. A. Bader, S. K. Muhammad, A. M. Jabbar, K. H. Abass, S. S. Chiad, N. F. Habubi, J. Nanostruct, 10(4): 744-750, (2020)

[48] O. M. Abdulmunem, A. M. Jabbar, S. K. Muhammad, M. O. Dawood, S. S. Chiad, N. F. Habubi, Journal of Physics: Conference Series,1660 (1), 012055 (2020); https://doi.org/10.1088/1742-6596/1660/1/012055
[49] M. S. Almomani, N. M. Ahmed, M. Rashid, M. A. Almessiere, A. S. Altowyan, Mater. Chem. Phys. 258, 123935 (2021); https://doi.org/10.1016/j.matchemphys.2020.123935
[50] H. Dang, E. Ososanaya, N. Zhang, Opt. Mater. 132, 112721 (2022); https://doi.org/10.1016/j.optmat.2022.112721
[52] E. H. Hadi, M. A. Abbsa, A. A. Khadayeir, Z. M. Abood, N. F. Habubi, and S.S. Chiad, Journal of Physics: Conference Series, 1664 (1), 012069 (2020); https://doi.org/10.1088/1742-6596/1664/1/012069
[53] Md.F. Rahman, Md.M. Alam Moon, Md.H. Ali, et al., Optical Materials, 117, 111136 2021; https://doi.org/10.1016/j.optmat.2021.111136
[47] S. K. Panda, S. Chakrabarti, A. Ganguly, and S. ChLidhuri, Journal of Nanoscience and Nanotechnology, 5, 459–465 (2005); https://doi.org/10.1166/jnn.2005.068
[48] Khadayeir, A. A., Hassan, E. S., Mubarak, T. H., Chiad, S.S., Habubi, N. F., Dawood, M.O., Al-Baidhany, I. A., Journal of Physics: Conference Series, 1294 (2) 022009(2019); https://doi.1088/1742-6596/1294/2/022009
[49] A. J. Ghazai, O. M. Abdulmunem, K. Y. Qader, S. S. Chiad, N. F. Habubi, AIP Conference Proceedings 2213 (1), 020101 (2020); https://doi.org/10.1063/5.0000158
[50] H. A. Hussin, R. S. Al-Hasnawy, R. I. Jasim, N. F. Habubi, S. S. Chiad, Journal of Green Engineering, 10(9), 7018-7028 (2020); https://doi.org/10.1088/1742-6596/1999/1/012063
[51] S. S. Chiad, H. A. Noor, O. M. Abdulmunem, N. F. Habubi, M. Jadan, J. S. Addasi, Journal of Ovonic Research, 16 (1), 35-40 (2020). https://doi.org/10.15251/JOR.2020.161.35
[52] H. T. Salloom, E. H. Hadi, N. F. Habubi, S. S. Chiad, M. Jadan, J. S. Addasi, Digest Journal of Nanomaterials and Biostructures, 15 (4), 189-1195 (2020); https://doi.org/10.15251/DJNB.2020.154.1189
[53] R. S Ali, N. A. H. Al Aaraji, E. H. Hadi, N. F. Habubi, S. S. Chiad, Journal of Nanostructuresthis link is disabled, 10(4), 810–816 (2020); https://doi: 10.22052/jns.2020.04.014
[54] S. K. Muhammad, N. D. M. Taqi, S. S. Chiad, K. H. Abass, N. F. Habubi, Journal of Green Engineering, 11(2), 1287-1299 (2021).
[55] A. A. Abdul Razaq, F. H. Jasim, S. S. Chiad F. A. Jasim, Z. S. A. Mosa , Y. H. Kadhimd, Journal of Ovonic Research, 20 (2), 131 – 141 (2024); https://doi.org/10.15251/JOR.2024.202.131
[56] E. S. Hassan, D. M. Khudhair, S. K. Muhammad, A. M. Jabbar, M.O. Dawood, N. F. Habubi, S. S. Chiad, Journal of Physics: Conference Series ,1660 (1) 1660 012066 (2020); https://doi.org/10.1088/1742-6596/1660/1/012066
[57] M. A. Kamran , T. Alharbi, Journal of Science: Advanced Materials and Devices,7, 100464 (2022); https://doi.org/10.1016/j.jsamd.2022.100464
[58] E.W. David, Sensors and Actuators B, 57, 1-16 (1999); https://doi.org/10.1016/S0925-4005(99)00133-1
[59] A. Giberti, D. Casottia, G. Cruciani, et al ., Sensors and Actuators B, 207, 504-510 (2014); https://doi.org/10.1016/j.snb.2014.10.054